B. Stothers, and A. L. Ternay, Jr., *J. Am. Chem. Soc.*, **92**, 5912 (1970).
(28) Isomer assignment was made on the basis of these values, together with the fact that Eu(fod)$_3$ causes substantially greater downfield shifts of H_{4a} in one isomer (assigned trans).
(29) An additional possibility is a rapid boat-to-boat inversion which could produce a comparable homoallylic coupling constant. However, if one substituent can be accommodated by a planar 1,4-cyclohexadiene (i.e., compound **2**), presumably a second could be accommodated similarly, provided it is on the other side of the ring.
(30) M. E. Kuehne and B. F. Lambert, *J. Am. Chem. Soc.*, **81**, 4278 (1959); *Org. Synth.*, **43**, 23 (1963).
(31) Attempts at complete NMR analysis with shift reagents were unsuccessful with this compound.
(32) J. C. Marshall, K. C. Erickson, and T. K. Folsom, *Tetrahedron Lett.*, 4011 (1970).
(33) Structure was assigned to this dihydro isomer, since only one bridgehead proton showed significant coupling and there are only two vinylic protons which are shifted downfield. In addition, uv shows conjugation.

Proton Magnetic Shielding Tensors from Spin-Rotation Measurements on H_2CO and NH_3

S. G. Kukolich

Contribution from the Department of Chemistry, The University of Arizona, Tucson, Arizona 85721. *Received February 7, 1975*

Abstract: The spin-rotation tensor for H_2CO was obtained from very high resolution beam maser measurements of rotational transitions. Spin-rotation tensor elements are $M_{aa} = -4.12 \pm 0.36$ kHz, $M_{bb} = 2.45 \pm 0.32$ kHz, and $M_{cc} = -2.10 \pm 0.34$ KHz in the principal axis system. These results are combined with previous molecular orbital calculations of diamagnetic shielding to obtain total absolute shielding tensor elements of $\sigma_{aa} = 15.9$, $\sigma_{bb} = 40.7$, and $\sigma_{cc} = -1.7$ ppm and an average shielding of 18.3 ppm with uncertainties of ±2 ppm or better. A similar analysis is carried out for NH_3. Spin-rotation tensors and shielding tensors are given for proton and nitrogen sites with estimated accuracy better than 1 ppm. For NH_3 $\sigma_{zz}(H) = 26.5$ ppm and $\bar{\sigma}(H) = 31.2$ ppm. The absolute shielding scale is discussed.

The average of the diagonal elements of the magnetic shielding tensors, more commonly known as the "chemical shift", has been extremely useful in structure determinations and characterizing particular types of bonding in functional groups. Since there are relatively large changes in shielding as the field direction is changed relative to molecular axes, a better understanding of magnetic shielding can be obtained from the shielding tensor. Shielding tensors have been obtained previously by orienting molecules in liquid crystals,[1] using multiple-pulse techniques on single crystals,[2] or molecular beam Zeeman measurements.[3,4] Relatively few experiments have yielded accurate shielding tensors or quadrupole coupling tensors using liquid crystal techniques. Results which are in good agreement with other measurements were obtained for linear or symmetric top molecules.[1] Difficulties appear to arise in establishing the order parameter. This problem is much more serious for asymmetric tops since the "orientation" axis is often not known and two-order parameters must be specified. Excellent results have been obtained from the multiple pulse measurements for larger molecules which may be frozen into rigid crystals and do not contain nuclei with quadrupole moments. Occasionally there are problems with this technique in determining the direction of shielding tensor axes relative to the bond directions. Direct measurements of shielding tensors for ^{19}F and ^{13}C have been obtained from high resolution molecular Zeeman measurements on molecular beams. These measurements are limited to a few small molecules with favorable magnetic and electric moments.

It was shown by Ramsey[5] that the magnetic shielding tensor for diatomic molecules could be separated into diamagnetic and paramagnetic parts. The diamagnetic part is expressed as first-order matrix elements between ground-state wave functions. The paramagnetic part depends on second-order terms for the mixing of excited electronic states having nonzero orbital angular momentum with the ground state. This type of treatment for diatomics was extended to symmetric-top and asymmetric-top molecules by Flygare[6] and coworkers. The diamagnetic terms may be easily and accurately obtained from ab initio molecular orbital calculations. The paramagnetic terms are very difficult to calculate and accuracy is poor. The paramagnetic terms, however, are related to electron contributions to the spin-rotation tensor by a numerical constant. This suggests that accurate magnetic shielding tensors may be obtained by combining calculated diamagnetic terms with paramagnetic terms from spin-rotation measurements. This method was used previously for fluorine shielding tensors.[7,8]

Formaldehyde rotational transitions were observed using a beam maser by Takuma, Shimizu, and Shimoda,[9] by Thaddeus, Krisher, and Loubser,[10] by Krupnov and Skvortsov,[11] and by Shigenari.[12] More accurate measurements on $J = 1$ and $J = 2$ K-type doublets were reported by Tucker, Tomasevich, and Thaddeus.[13]

The resolution of the two-cavity maser spectrometer[14] using Ramsey's method of separated oscillating fields is significantly better than the resolution of single cavity masers. Measurements of the 1_{10}-1_{11} transition of H_2CO using a two-cavity maser were reported previously.[15]

Experimental Section

The two-cavity maser spectrometer was described previously.[14,15] For the present measurements the beam was produced with a 0.1 mm diameter stainless steel nozzle. Formaldehyde vapor was obtained by heating a paraformaldehyde-silicone oil slurry. The upper state was focussed using a quadrupole lens. Two OFHC copper cavities excited in the TM_{010} mode were used to observe resonances. The cavity separation was 76 cm and the width of the central peak of the resonance pattern was 390 Hz. A "fast scan" recorder trace of all observed components is shown in Figure 1. The upper trace (a) is the "single-cavity" spectrum and the lower trace (b) was obtained using the two-cavity maser. Both spectra are shown as derivatives of the emission spectrum due to the frequency modulation with lock-in detection used in the apparatus.

Spin-Rotation Tensor

The strongest lines of the $2_{11} \rightarrow 2_{12}$ transition and our previous data on the $1_{10} \rightarrow 1_{11}$ transition were analyzed to determine the spin-rotation tensor and spin-spin interac-

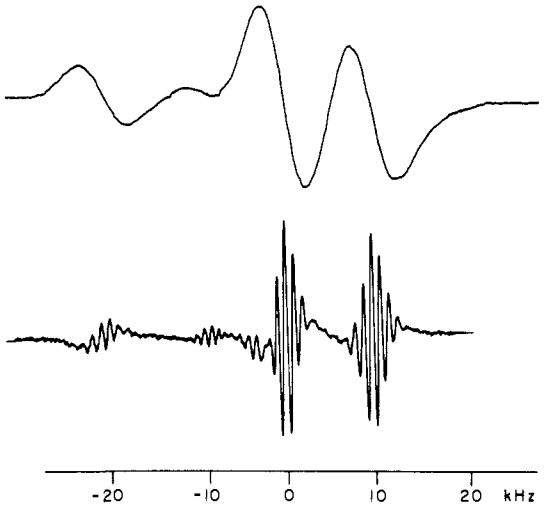

Figure 1. Recorder traces of single-cavity (a) and two-cavity (b) spectra of the $2_{11} \rightarrow 2_{12}$ transition in H_2CO. The frequency scale is relative to the line center at 14,488,479. kHz.

tion strength. The Hamiltonian for this problem was described previously.[15] The results of a least-squares fit using the three diagonal elements of the spin-rotation tensor and spin-spin interaction strength as adjustable parameters are given in Table I. The standard deviation for the fit of 0.7 kHz was larger than the average statistical uncertainty in the individual like measurements of 0.13 kHz. Parameters determined from this analysis are given in Table II. The spin-rotation parameters M_{gg} were in reasonably good agreement with previous work.[13] The spin-spin interaction strength $S = \mu_1\mu_2/r^3$ is smaller than the value 17.91 kHz calculated from the molecular geometry including the most important distortion term. Indicated error limits are one standard deviation only.

The electronic contributions to the spin-rotation tensor are obtained by subtracting nuclear contributions from the total experimental spin-rotation tensor elements.

Magnetic Shielding Tensor

The diagonal elements of the shielding tensor in the principal rotational axis system are expressed as the sum of the diamagnetic and paramagnetic contributions.

$$\sigma_{xx} = \sigma_{xx}^{d} + \sigma_{xx}^{p}$$

The paramagnetic contribution to the xx component of the shielding tensor is directly related to the xx component of the spin-rotation tensor by subtracting a term representing nuclear contributions to the spin-rotation interaction

$$\sigma_{xx}^{p} = \frac{M_p}{2mg_I}\frac{M_{xx}}{G_{xx}} - \frac{e^2}{2mc^2}\sum_n{}' \frac{Z_n}{r_n^3}(y_n^2 + z_n^2)$$

where M_p is the proton mass, m is the electron mass, g_I is the nuclear g value, and M_{xx}/G_{xx} is the ratio of spin-rotation strength to rotational constant in the x direction. The molecular geometry of H_2CO is given by Oka.[16] The diamagnetic contributions to the shielding tensor were calculated by Neumann and Moskowitz.[17] This was a Hartree-Fock, SCF calculation and appears to be the best ab initio calculation on H_2CO. They also calculated nuclear contributions to spin-rotation tensor elements and we will use their results since they were obtained for the same geometry as electronic contributions to diamagnetic terms. Paramagnetic, diamagnetic, and total shielding tensor elements are listed in Table III. For the paramagnetic term the listed uncertainty includes only the contribution from spin-rotation terms. There may be larger errors due to errors in geometry

Table I. Results of the Least-Squares Fit to $J = 1$ and $J = 2$ Hyperfine Structure in H_2CO[a]

J	F_U	F_L	Data	Calculated	Deviation
1	1	0	−18.67	−18.63	−0.04
1	0	1	—1.17	−1.44	0.27
1	2	2	−0.46	−0.37	−0.09
1	2	1	3.96	4.00	−0.04
1	1	2	6.46	6.59	−0.14
1	1	1	11.08	10.96	0.12
2	1	1	−20.16	−20.07	−0.09
2	1	2	−7.88	−7.88	0.00
2	3	3	0.95	0.77	0.19
2	2	2	10.82	10.96	−0.14

[a] $J = 1$ line center at 4, 829, 659.9 kHz and $J = 2$ line center at 14,488,479.1 kHz. Frequencies in kHz relative to line centers. Standard deviation for the fit = 0.7 kHz.

Table II. Hyperfine Structure Parameters and Line Centers for H_2CO

Parameter	Value, kHz
M_{aa}	−4.12 ± 0.36
M_{bb}	2.45 ± 0.32
M_{cc}	−2.10 ± 0.34
S	17.65 ± 0.14
$1_{10} \rightarrow 1_{11}$ center	4,829,659.9 ± 0.2
$2_{11} \rightarrow 2_{12}$ center	14,488,479.1 ± 0.3

Table III. Paramagnetic (σ_{xx}^{p}), Diamagnetic (σ_{xx}^{d}), and Total (σ_{xx}) Shielding Tensor Components along the Principal Rotational Axes in H_2CO[a]

Axis	σ_{xx}^{p}	σ_{xx}^{d}	σ_{xx}
a	−76.7 ± 0.2	92.6	15.9
b	−54.0 ± 1.4	94.7	40.7
c	−148.8 ± 1.6	147.1	−1.7
Av	−69.3 ± 1.2	111.5	18.3

[a] Units are ppm. The listed uncertainty is only the contribution from uncertainty in the spin–rotation term.

but these should be cancelled by corresponding errors in diamagnetic terms. Diamagnetic shielding tensor components obtained from the semiempirical atom-dipole model[18] are in reasonably good agreement with results from the ab initio calculation.[17] We note from Table III that the largest shielding anisotropy is with respect to the b axis with $2\sigma_{bb} - \sigma_{aa} - \sigma_{cc} = 67.2$ ppm. This is well below the upper limit of 200 ppm established from high-resolution microwave Zeeman measurements.[19] It is difficult to place error limits on the diamagnetic contribution σ_{xx}^{d} but we would estimate that they are accurate to within a few parts per million. The diamagnetic shielding terms are only dependent on ground state wave functions and not very sensitive to the choice of basis set. It was pointed out by Ramsey[20] that there exists a linear relationship between $\Sigma M_{xx}I_{xx}$ and chemical shifts.[20] This was extended by the Flygare-Goodisman[21] model which relates the average spin-rotation contribution to shielding to the average shielding

$$\sigma_{av}^{sr}(\text{molecule}) + \sigma_{av}(\text{free atom}) = \sigma_{av}(\text{molecule})$$

where $\sigma_{av}^{sr} = (M_p/6mg_I)\Sigma\, M_{xx}/G_{xx}$; for H_2CO $\sigma_{av}^{sr} = 0.8$ ppm, and σ_{av}(molecule) = 18.3. This would yield σ_{av}(free atom) = 19.1 ppm. For hydrogen this value may be accurately calculated[22] from $\langle 1/r \rangle$ to be 17.75 ppm. An additional term included in a more recent treatment[18] could possibly improve the model. The simplified form above is seen to be in error by only slightly more than 1 ppm.

NH_3 Shielding Tensors

A similar procedure may be used to calculate the proton and nitrogen shielding tensors in NH_3. High resolution

Table IV. Results of Least-Squares Fit of Observed Spin–Rotation Constants for Observed Transitions in $^{15}NH_3$[a]

J	K	C^H(exptl)	C^H(calcd)	C^N(exptl)	C^N(calcd)
1	1	−18.362	−18.382	−9.496	−9.485
2	2	−18.583	−18.577	−9.437	−9.447
3	3	−18.711	−18.674	−9.404	−9.428
4	4	−18.751	−18.732	−9.424	−9.416
5	5	−18.770	−18.771	−9.418	−9.408
5	5	−18.779	−18.820	−9.404	−9.399

[a] Exptl and calcd are experimental and calculated values in kHz.

Table V. Results of Least-Squares Fit of Spin–Rotation Constants for Observed Transitions in $^{14}NH_3$[a]

J	K	C^H(exptl)	C^H(calcd)	C^N(exptl)	C^N(calcd)
3	1	−17.829	−17.839	6.753	6.758
2	1	−17.939	−17.948	6.756	6.752
4	2	−17.984	−17.992	6.749	6.750
5	3	−18.164	−18.124	6.746	6.743
1	1	−18.379	−18.387	6.729	6.729
2	2	−18.611	−18.606	6.720	6.718
3	3	−18.709	−18.716	6.715	6.712
4	4	−18.781	−18.782	6.712	6.709
5	5	−18.825	−18.826	6.698	6.706

[a] Values in kHz

beam maser measurements on a large number of rotational states in $^{14}NH_3$ and $^{15}NH_3$ were reported by Kukolich,[23] Kukolich and Wofsy,[24] and Ruben and Kukolich.[25] Some anomalies in the earlier work were removed in the theoretical analysis by Hougen[26] which included a more complete and careful theoretical treatment and inclusion of a new distortion effect on quadrupole coupling. The hydrogen and nitrogen spin-rotation strengths for a given J,K rotational state may be written on the form[24]

$$C^H(J,K) = -(M_{xx}^H + M_{yy}^H)/2 - (2M_{zz}^H - M_{xx}^H - M_{yy}^H)K^2/2J(J+1) + (M_{xx}^H - M_{yy}^H)\delta_{K1}(-1)^{J+v}/2$$

$$C^N(J,K) = -M_{aa}^N - (M_{zz}^N - M_{aa}^N)K^2/J(J+1)$$

The z axis is the C_3 symmetry axis, the y axis is perpendicular to the N-H band and parallel to the hydrogen plane, and the x axis is parallel to the hydrogen plane and in the plane of the z axis and N-H bond (see Figure 2, ref 24). $M_{aa} = (M_{xx} + M_{yy})/2$ and represents the component perpendicular to the z axis. v represents the inversion quantum number. The results of fitting spin-rotation constants $C(J,K)$ for measured transitions to the above expressions are given in Tables IV and V. The spin-rotation tensor elements are listed in Table VI. The term not listed in the tables is $M_{xx}^H - M_{yy}^H = -28.98 \pm 0.03$ based on four measurements of $K = 1$ transitions. It is interesting to note that perpendicular and parallel components of hydrogen and nitrogen spin-rotation tensors are nearly equal but the perpendicular and parallel rotation constants and electronic structure are quite different.

The paramagnetic shielding tensor elements for hydrogen and nitrogen calculated from the above spin-rotation tensors are listed in Table VII. The hydrogen spin-rotation tensor elements are $M_{xx} = 3.28$, $M_{yy} = 32.26$, $M_{zz} = 19.01$ kHz. Rotational constants and structure were given by Benedict and Plyler.[27] The best structure is probably the $v = 0$ structure,[27] but it is very important to calculate nuclear spin-rotation terms using the same structure as that used for calculating diamagnetic terms. High-accuracy Hartree-Fock calculations were reported by Laws, Stevens, and Lipscomb[28] and later refined somewhat by Stevens.[29] We will use the results of the diamagnetic shielding calculations listed in Table VI of ref 28, equilibrium column, corresponding to a structure with a proton ($x = 1.754$, $z = 0.703$ au) relative to the nitrogen atom. This structure is somewhat closer to the experimental[27] $v = 0$ structure than others used and a more complete set of proton shielding parameters is given. The average absolute proton shielding is $\bar{\sigma}(H) = 31.2$ ppm and the average absolute nitrogen shielding $\bar{\sigma}(N) = 264.5$ ppm. The nitrogen shielding anisotropy is quite large with $\sigma_{zz} - \sigma_{aa} = -40.3$ ppm. The shielding is greater in the plane of the molecule as observed previously for fluorine.[4] This is also the case for the protons in NH_3 where the shielding anisotropy is $\sigma_{zz} - \sigma_{aa} = 7$ ppm. We note that the anisotropy between x and y directions is quite large but this would not be observable in most experiments on ammonia due to the equivalence of axes perpendicular to the symmetry axis. In substituted amines these directions would no longer be equivalent. Here we have $\bar{\sigma}$(molecule) − $\bar{\sigma}^{sr}$ = 19.1 ppm, exactly the value obtained for H_2CO and slightly larger than the free atom absolute shielding.

Table VII. Paramagnetic, Diamagnetic, and Total Shielding Tensor Components along Principal Rotational Axes in NH_3[a]

	Axis	σ_{gg}^p(H)	σ_{gg}^d(H)	σ_{gg}	σ_{gg}^{sr}(H)
Hydrogen	z	−85.67	112.18	26.51	16.82
	a	−55.10	88.60	33.50	9.80
	x	−16.23	57.39	41.16	1.81
	y	−93.98	119.82	25.84	17.78
Nitrogen	z	−118.27	355.97	237.70	−81.86
	a	−75.96	353.92	277.96	−51.90

[a] The a axis represents the average of components perpendicular to the symmetry axis z so $\sigma_{aa} = (\sigma_{xx} + \sigma_{yy})/2$, etc. Units ppm.

Discussion

Absolute proton magnetic shielding values of $\bar{\sigma} = 18.3 \pm 2.0$ ppm and $\bar{\sigma} = 31.2 \pm 1.0$ ppm were obtained for H_2CO and NH_3 in the gas phase. These values, particularly the NH_3 shielding, may be useful in establishing or checking an absolute shielding scale. The absolute shielding of H_2 was determined to be 26.43 ± 0.60 ppm by Myint et al.[30] In the gas phase[31] $\bar{\sigma}(NH_3) = 4.25$ relative to H_2. The resulting value $\bar{\sigma}(NH_3) = 30.7 \pm 0.6$ is in agreement with the above value from the book by Carrington and McLachlan[32] of $\bar{\sigma}(NH_3) = 30.85$ ppm. The same reference[32] lists the ^{14}N average shielding in NH_3 as 266 ppm and we obtain $\bar{\sigma}_N(NH_3) = 264.5$ ppm. The accuracy of the results for the average shielding provides some degree of confidence in the accuracy of shielding tensors. Changes in proton chemical shifts in ammonia due to isotopic substitution are very small[33] (>0.1 ppm) so we do not expect vibrational corrections to be important.

Table VI. Spin–Rotation Tensor Elements Determined from Least-Squares Fits[a]

	$^{15}NH_3$		$^{14}NH_3$	
Axis g	M_{gg}^N	M_{gg}^H	M_{gg}^N	M_{gg}^H
a(perpendicular)	9.60 ± 0.02	17.80 ± 0.03	−6.764 ± 0.005	17.73 ± 0.02
z(parallel)	9.37 ± 0.02	18.97 ± 0.03	−6.695 ± 0.005	19.05 ± 0.02

[a] Values in kHz; a perpendicular to symmetry axis and z parallel to symmetry axis.

Average magnetic shielding values for NH_3 and H_2CO have recently been calculated from molecular orbital theory by Ditchfield.[34] These calculated values for hydrogen are $\bar{\sigma}(H_2CO) = 22.3$ and $\bar{\sigma}(NH_3) = 33.6$ ppm and for nitrogen $\sigma(NH_3) = 267.8$ ppm. The agreement with our above results is reasonably good in view of the difficulty of ab initio calculations of the paramagnetic term.

Acknowledgment. The writer wishes to thank Dr. Michael Barfield for helpful discussion on this work. The support of the National Science Foundation, Structural Chemistry Section, was greatly appreciated.

References and Notes

(1) P. K. Bhattacharyya and B. P. Dailey, *J. Chem. Phys.*, **59**, 5820 (1973).
(2) S. Pausak, J. Tegenfeldt, and J. S. Waugh, *J. Chem. Phys.*, **61**, 1338 (1974); P. Van Hecke, T. C. Weaver, B. L. Neff, and J. S. Waugh, *ibid.*, **60**, 1668 (1974), and references cited therein.
(3) F. H. De Leeuw and A. Dymanus, *Chem. Phys. Lett.*, **7**, 288 (1970).
(4) S. G. Kukolich and A. C. Nelson, *J. Chem. Phys.*, **56**, 4446 (1972).
(5) N. F. Ramsey, *Phys. Rev.*, **78**, 699 (1950); "Molecular Beams", Oxford University Press, London, 1956, Chapter 6.
(6) W. H. Flygare, *J. Chem. Phys.*, **41**, 793 (1964); W. Hüttner and W. H. Flygare, *ibid.*, **47**, 4137 (1967).
(7) S. G. Kukolich, T. H. S. Wang, and D. J. Ruben, *J. Chem. Phys.*, **58**, 5474 (1973).
(8) J. H. S. Wang and S. G. Kukolich, *J. Am. Chem. Soc.*, **95**, 4138 (1973).
(9) H. Takuma, T. Shimizu, and K. Shimoda, *J. Phys. Soc. Jpn.* **14**, 1595 (1959); **15**, 2036 (1960); **16**, 309 (1961).
(10) P. Thaddeus, L. C. Krisher, and J. H. N. Loubser, *J. Chem. Phys.*, **40**, 257 (1964).
(11) A. F. Krupnov and V. A. Skvortsov, *Sov. Phys. JETP (Engl. Transl.)*, **40**, 257 (1964).
(12) T. Shigenari, *J. Phys. Soc. Jpn.*, **23**, 904 (1967).
(13) K. D. Tucker, G. R. Tomasevich, and P. Thaddeus, *Astrophys. J.*, **169**, 429 (1971); **174**, 463 (1972).
(14) S. G. Kukolich, *Phys. Rev.*, **138**, A1322 (1965).
(15) S. G. Kukolich and D. J. Ruben, *J. Mol. Spectrosc.*, **38**, 130 (1971).
(16) T. Oka, *J. Phys. Soc. Jpn.*, **15**, 2279 (1960); **18**, 1174 (1963).
(17) D. B. Neumann and J. W. Moskowitz, *J. Chem. Phys.*, **50**, 2216 (1969).
(18) T. D. Gierke and W. H. Flygare, *J. Am. Chem. Soc.*, **94**, 7277 (1972).
(19) S. G. Kukolich, *J. Chem. Phys.*, **54**, 8 (1971).
(20) N. F. Ramsey, *Am. Sci.*, **49**, 509 (1961).
(21) W. H. Flygare and J. Goodisman, *J. Chem. Phys.*, **49**, 3122 (1968).
(22) S. C. Wofsy, J. S. Muenter, and W. Klemperer, *J. Chem. Phys.*, **55**, 2014 (1971).
(23) S. G. Kukolich, *Phys. Rev.*, **138**, A1322 (1965); **156**, 83 (1967); **172**, 59 (1968).
(24) S. G. Kukolich and S. C. Wofsy, *J. Chem. Phys.*, **52**, 5477 (1970).
(25) D. J. Ruben and S. G. Kukolich, *J. Chem. Phys.*, **61**, 3780 (1974).
(26) J. T. Hougen, *J. Chem. Phys.*, **57**, 4207 (1972).
(27) W. S. Benedict and E. K. Plyler, *Can. J. Phys.*, **35**, 1235 (1957).
(28) E. A. Laws, R. M. Stevens, and W. N. Lipscomb, *J. Chem. Phys.*, **56**, 2029 (1972).
(29) R. M. Stevens, *J. Chem. Phys.*, **61**, 2086 (1974).
(30) T. Myint, D. Kleppner, N. F. Ramsey, and H. G. Robinson, *Phys. Rev. Lett.*, **17**, 405 (1966).
(31) J. A. Pople, W. G. Schneider, and H. J. Bernstein, "High-Resolution Nuclear Magnetic Resonance", McGraw-Hill, New York, N.Y., 1959, Chapter 5.2.
(32) A. Carrington and A. D. McLachlan, "Introduction to Magnetic Resonance", Harper and Row, New York, N.Y., 1967, Chapter 5.4.
(33) R. A. Bernstein and H. Batiz-Hernandez, *J. Chem. Phys.*, **40**, 3446 (1964).
(34) R. Ditchfield, *Mol. Phys.*, **27**, 789 (1974).

High Resolution Nuclear Magnetic Resonance Studies of Chemical Reactions Using Flowing Liquids. Investigation of the Kinetic and Thermodynamic Intermediates Formed by the Attack of Methoxide Ion on 1-X-3,5-dinitrobenzenes[1]

Colin A. Fyfe,*[2] Michael Cocivera, and Sadru W. H. Damji

Contribution from the Guelph-Waterloo Centre for Graduate Work in Chemistry, Chemistry Department, University of Guelph, Guelph, Ontario, Canada N1G 2W1.
Received February 14, 1975

Abstract: High resolution nuclear magnetic resonance spectroscopy in a flowing system has been used to investigate both the kinetic and the thermodynamic distributions of the isomeric complexes formed by the attack of methoxide ion on 1-X-3,5-dinitrobenzenes (where X = CN, CF_3, $COOCH_3$, $COOCH_2CH_3$) by the direct observation of these species at various reaction times in a flowing, chemically reacting system. In all cases a *mixture* of the two species is formed initially under kinetic control and the conversion from kinetically to thermodynamically controlled distributions occurs in less than 2 sec for all the compounds investigated. The results are compared with data on the reactions from previous uv–visible spectroscopic measurements and a reinterpretation of these data is given.

The various spectroscopic techniques used for kinetic measurements of chemical reactions all have their unique advantages and disadvantages. Thus, uv–visible spectroscopy has the advantage that it is a very sensitive technique and it is by far the most widely used method for making flow and stopped-flow kinetic measurements in reacting chemical systems. It does, however, have a severe disadvantage in that it is relatively nondiagnostic, the results leaving the identity of many observed species uncertain and in some cases depending on spectral assignments which may directly affect the interpretation of the kinetic data. Ir spectroscopy is less sensitive but is somewhat more diagnostic, depending on the presence of specific, often identifiable groupings of atoms in the molecule. It is used only infrequently, however, mainly due to its lack of sensitivity. ESR combines a high degree of sensitivity with a considerable amount of diagnostic character but is obviously applicable only to a restricted class of compounds. However, it has found wide application for radical reactions and is often used where the species observed are in a flowing chemically reacting system, permitting the observation of relatively short-lived species.

High-resolution nuclear magnetic resonance spectroscopy is much less sensitive than uv–visible spectroscopy (often by several orders of magnitude) but has a great advantage as a diagnostic tool and can provide much more information